North-South disparity in impact of climate change on “outdoor days”

Yeon-Woo Choi, Muhammad Khalifa, and Elfatih A. B. Eltahir

Supplementary Information

Text S1. The concept of loss and damage by climate change.

Text S2. Online interactive platform for “outdoor days”.

Table S1. List of CMIP5 and CMIP6 models used in this study.

Table S2. Summary of previous studies that analyzed mild weather at different spatial scales.

Table S3. Observed change (1991-2020 minus 1961-1990) in the number of outdoor days with different definitions and variables. T and TW denote dry-bulb temperature and wet-bulb temperature, respectively.

Figure S1. Definition of the three components of climate risk. Definitions are obtained from IPCC (2022).

Figure S2. Observed and simulated outdoor days. Spatial distributions of the number of annual outdoor days (days per year) for the period 1976-2005, derived from the ERA5 (top), ensemble mean of 21 NEX-GDDP-CMIP5 GCMs (middle), and ensemble mean of 32 NEX-GDDP-CMIP6 GCMs (bottom).

Figure S3. Probability Mass Functions (PMF) of (a) 90th and (b) 10th percentiles of daily dry-bulb temperature in densely populated areas across the world (areas with a population density above 10 persons per square kilometer) over the period 1976–2005. The results are derived from ERA5.

Figure S4. Four different heat-stress categories provided by the US National Weather Service. Wet-bulb temperature as a function of dry-bulb temperature and relative humidity is indicated.

Figure S5. The latitudinal population distribution (unit: million people) in 2000.

Figure S6. Global distribution of temperature. a) Climatology of annual mean temperature for the period 1959-2021. b) Change in annual mean temperature in 1991–2020 with respect to 1961-1990. These global maps are derived from ERA5.

Figure S7. Global maps of GDP, CO_2 emission, and population density. Spatial distributions of a) GDP per capita (USD), b) CO_2 emissions per capita, and c) population density (persons per square kilometer).

Figure S8. Temporal evolution of outdoor days derived from NEX-GDDP-CMIP5 models. Time series of the number of annual outdoor days (days per year) over residential areas (assumed, areas with a population density above 1 person per square kilometer) derived from 21 NEX-GDDP-CMIP5

GCMs under the historical and RCP8.5 scenarios. Thick solid blue line indicates an ensemble mean of models. Horizontal black and blue lines denote the 1976-2005 mean and the 2071-2100 mean, respectively. Difference (2071–2100 minus 1976–2005) in the number of outdoor days is represented in each plot. The background image was obtained from NASA Visible Earth.

Figure S9. Temporal evolution of population. Time series of population (million persons) over residential areas (assumed, areas with a population density above 1 person per square kilometer) derived from the SSP5 scenario. Horizontal black and blue lines denote the 2000-2029 mean and the 2071-2100 mean, respectively. Difference (2071–2100 minus 2000–2029) in population is represented in each plot. The background image was obtained from NASA Visible Earth.

Figure S10. Projected change in precipitation. Spatial distribution of change in annual mean precipitation (%) in 2071-2100 with respect to 1976-2005, derived from 32 NEX-GDDP-CMIP6 GCMs. Superimposed hatching indicates that more than 80% of models agree on the sign of the change. Zonal-mean change is indicated in the right panel. Thick solid blue line in the right panel indicates an ensemble mean of models.

Figure S11. Normalized change in the number of annual outdoor days with different definitions. Normalized change in the number of annual outdoor days in 2071–2100 with respect to 1976-2005. The changes are normalized by the 1976-2005 mean. Various definitions considered are indicated in each plot. Dry-bulb temperature and precipitation are indicated by T and PR, respectively. These global maps are derived from EC-Earth3-Veg-LR.

Figure S12. Temporal evolution of CO_2 emission and GDP. Time series of (top) CO_2 emissions per capita and (bottom) GDP per capita (USD) for the United States, the European Union, Russia, Brazil, Nigeria, and India. The GDP data for European Union (Russia) is only available since 1970 (1989).

Text S1. The concept of loss and damage by climate change

The concept of Loss and Damage (L&D) in climate change refers to the negative impacts of climate change that cannot be prevented through mitigation and adaptation efforts (van der Geest and Warner 2020). Although the L&D concept has been intensively discussed in numerous international conventions related to climate change, including the United Nations Warsaw International Mechanism for Loss and Damage and the Parsis Agreement, it is still one of the most challenging issues when it comes to definition, evidence, laws, and mechanisms (Boyd et al. 2021; Doelle and Seck 2020). Recently, this concept has received more attention in the global climate agenda (Boyd et al. 2021), mainly because of its importance and strong relevance to countries that are more vulnerable to climate change impacts (Pflieger 2023), which are mainly developing countries located in the tropical regions. The recent agreement on creating the Loss and Damage (L&D) fund during the 27th Conference of Parties (COP27) held in Egypt in November 2022 represents a substantial breakthrough in the international climate change policy to compensate countries vulnerable to climate change (Warner and Weisberg 2023). It calls for mobilizing financial resources to the L&D fund from a variety of sources, hence, minimizing some of the concerns of the developed countries.

Text S2. Online interactive platform for "outdoor days"

We have developed a flexible approach to defining outdoor days, which allows users to customize their criteria for defining outdoor days using various climate variables, including dry-bulb surface air temperature, wet-bulb surface air temperature, and rainfall. This approach is facilitated through our online interactive platform (https://eltahir.mit.edu/globaloutdoordays/). On the website, users can select a specific region of interest and choose variables that are important to their outdoor activities. Setting a preferred range for each variable is one of the important advantages of this tool. With these simple steps, users can see how the number of outdoor days in the selected region will change until the end of this century under the low and high emissions scenarios.

Table S1. List of CMIP5 and CMIP6 models used in this study.

	Models	Variable	Temporal resolution	Ensemble member
NEX-GDDP-CMIP5	ACCESS1-0, BNU-ESM, CCSM4, CESM1-BGC, CNRM-CM5, CSIRO-Mk3-6-0, CanESM2, GFDL-CM3, GFDL-ESM2G, GFDL-ESM2M, IPSL-CM5A-LR, IPSL-CM5A-MR, MIROC-ESM-CHEM, MIROC-ESM, MIROC5, MPI-ESM-LR, MPI-ESM-MR, MRI-CGCM3, NorESM1-M, bcc-csm1-1, inmcm4	Dry-bulb temperature	Daily	r1i1p1
NEX-GDDP-CMIP6	ACCESS-CM2, ACCESS-ESM1-5, BCC-CSM2-MR, CanESM5, CESM2-WACCM, CESM2, CMCC-ESM2, CNRM-CM6-1, CNRM-ESM2-1, EC-Earth3-Veg-LR, EC-Earth3, FGOALS-g3, GFDL-CM4, GFDL-ESM4, GISS-E2-1-G, HadGEM3-GC31-LL, HadGEM3-GC31-MM, IITM-ESM, INM-CM4-8, INM-CM5-0, IPSL-CM6A-LR, KACE-1-0-G, KIOST-ESM, MIROC-ES2L, MIROC6, MPI-ESM1-2-HR, MPI-ESM1-2-LR, MRI-ESM2-0, NESM3, NorESM2-LM, NorESM2-MM, UKESM1-0-LL	Dry-bulb temperature	Daily	r1i1p1f1
CMIP6	ACCESS-CM2, BCC-CSM2-MR, CMCC-CM2-SR5, CMCC-ESM2, EC-Earth3, KIOST-ESM, MIROC6, MPI-ESM1-2-HR, MPI-ESM1-2-LR, MRI-ESM2-0	Dry-bulb temperature, Dew-point temperature, Surface pressure	3-hourly	r1i1p1f1

Table S2. Summary of previous studies that analyzed mild weather at different spatial scales.

Author(s)	Term used, definition and variables used	Spatial coverage/resolution	Temporal coverage	Data used	Methods	Main results
Heng and Chow, (2019)	**Outdoor Thermal Comfort (OTC)** Neutral T Acceptable T Preferred (ideal) T	Local (Singapore urban park)	2013/2014	1537 Surveys	Surveys	Neutral T =26.2 ℃ Acceptable T= 21.6-31.6 ℃ Preferred (ideal) T= 24.2 ℃
Zhang (2016)	**Good weather**: Midrange temperature and little or no precipitation *Daily max. T < 25 ℃*	Local (Washington D.C and New York)	1960-1995	7000 social movement events 36 years of weather records from GHCN-Daily dataset	Logistic regression models	Violence occurs more frequently at social movement events when it is warmer
van der Wiel et al. (2017)	**Mild weather** is weather that is neither too hot, too cold, too humid nor rainy weather that could also be described as being pleasant. *Daily maximum air temperature= 18-30 ℃* *Daily total precipitation < 1mm* *Daily mean dewpoint temperature < 20 ℃*	Global (0.25° x 0.25°)	Up to 2100	CMIP5 MERRA-2 Human Population	High-resolution global climate model (HiFLOR)	A slight global mean decrease in the annual number of mild days projected both in the near future (−4 days per year, 2016–2035) and at the end of this century (−10 days per year, 2081–2100).
Zhang et al. (2022)	**Mild weather** is a positive and pleasant condition and is highly related to human outdoor activities. It is generally accepted that mild weather is closely related to thermal comfort conditions, which	National (China)	historical simulations (1980-2005) and future projections (2006–2099)	HadGEM2-ES, MPI-ESM-MR, and NorESM1-M	Comprehensive thermal comfort indices, and dynamically downscaled climate projections	Densely populated southeastern China will experience a robust decrease in mild weather relative to the current level.

	considers the aggregate effects of temperature, relative humidity, wind, and radiation on human thermal perception *Temperature* *Relative humidity* *Wind speed* *Sunshine duration*				produced by the Regional Climate Model version 4 (RegCM4)	
Hanlon et al. (2021)	**High impact weather** *Frost days: daily min. T < 0 ℃* *Icing days: daily min. T < 0 ℃* *Tropical nights: daily min. T > 20 ℃* *Summer days: daily max. T > 25 ℃* *Heating degree days: Daily mean T < 15.5 ℃* *Daily mean T > 22 ℃*	National (UK) 12 km	1981-2000	Ensemble of 12 RCMs	UKCP 12-km resolution regional climate model	Increases in the frequency of extremely hot days and nights
Lin et al. (2019)	**Mild weather:** day is considered as mild if the daily temperature-humidity index (THI) is between 17 and 25.4 for May–October or the wind chill index (WCI) is between -299 and - 100 for November–April *Temperature* *Relative humidity* *Wind speed* *Sunshine duration*	National (China)	1971-2014	Daily observations at a network of 2,060 meteorological stations	Clustering analysis	The annual number of mild days increased by 1.02% per decade (3.73 days per decade) during 1971–2014. They also found that most parts of China have been experiencing increasing mild weather in 1971–1998 but decreasing in 1998–2014

Wu et al. (2017)	**Comfortable days** Daily mean temperature (°C) Relative humidity (%) Wind spead (m s^{-1}) *Comfortable T = 17-25 (°C)*	National (China)	1961–2014	CN05.1	Determine of thermal sensations based on Effective Temperature (ET)	During the analysis period, the number of annual comfortable days shows an increasing trend when considering the China-wide average. However, the number of annual comfortable days during JJA decreases over warm areas.
Gao et al. (2018)	**Thermal comfort conditions** Daily mean temperature (°C) Relative humidity (%) Wind spead (m s^{-1}) *Comfortable T = 17-25 (°C)*	National (China)	1979–2098	Coupled Model Intercomparison Project Phase 5 (CMIP5)	RegCM4	Even a mid-level warming scenario is found to increase the thermal stress over China, although there is a strong geographical dependence
Day et al. (2021)	**Mild days** *Mild weather is defined as temperatures between 65 and 86 °F (18 and 30 °C).*	Local (Indiana, USA)	2020s, 2050s 2080s	Literature	Literature review	Climate change in Indiana will increase the number of hot and extremely hot days each summer, reducing the number of mild days. This will have direct and indirect impacts on tourism and recreation.
Spagnolo and de Dear (2003)	**Thermal comfort (Outdoor Standard Effective Temperature)** Thermal neutrality = 26.2 °C Air Temperature Relative humidity Global shortwave radiation	Local (Sydney, Australia)	1998-2000	Field measurements Questionnaire responses	Micro-meteorological sensors Survey	Comfort zone limits in outdoor areas are higher than those of indoor areas due to more variable environment and also the perceived lack of control

	Diffuse shortwave radiation Longwave radiation Velocity					over the outdoor environment.

Table S3. Observed change (1991-2020 minus 1961-1990) in the number of outdoor days with different definitions and variables. T and TW denote dry-bulb temperature and wet-bulb temperature, respectively.

	Globe	30S-30N	30N-60N	60N-90N
10℃ <= T <= 20℃	-0.3 (-0.7%)	-6.9 (-10.4%)	2.2 (2.2 %)	4.6 (15.0 %)
10℃ <= T <= 25℃	-3.9 (-4.2%)	-24.0 (-12.8%)	4.7 (3.5%)	5.4 (16.3%)
15℃ <= T <= 20℃	-0.4 (-1.5%)	-4.8 (-10.5%)	1.8 (3.9%)	1.8 (18.4%)
15℃ <= T <= 25℃	-4.0 (-5.8%)	-21.8 (-13.1%)	4.3 (5.4%)	2.6 (21.3%)
8℃ <= TW <= 15℃	-0.2 (-0.4%)	-6.7 (-7.8%)	2.5 (2.7%)	4.4 (16.9%)

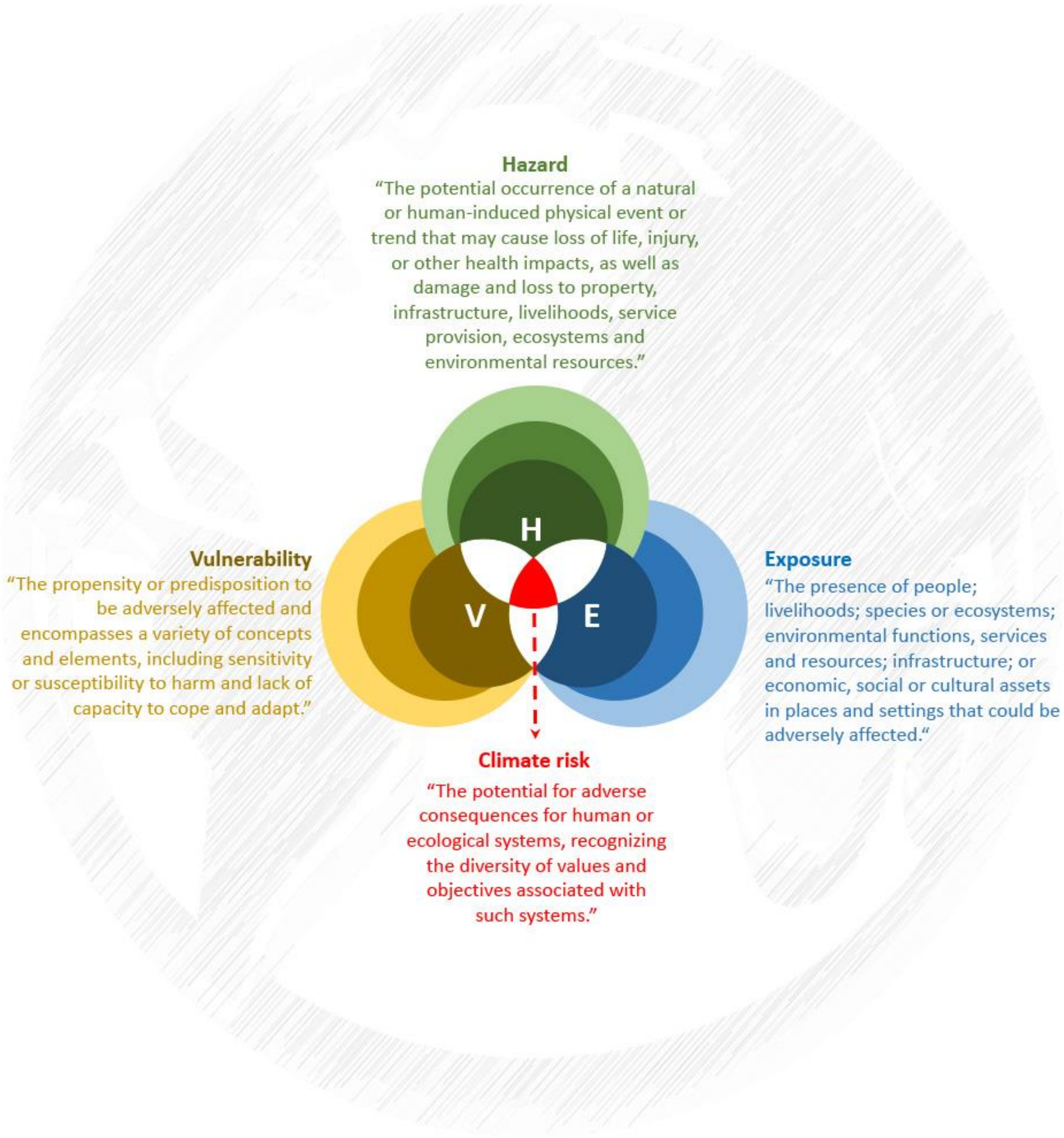

Fig. S1. Definition of the three components of climate risk. Definitions are obtained from IPCC (2022).

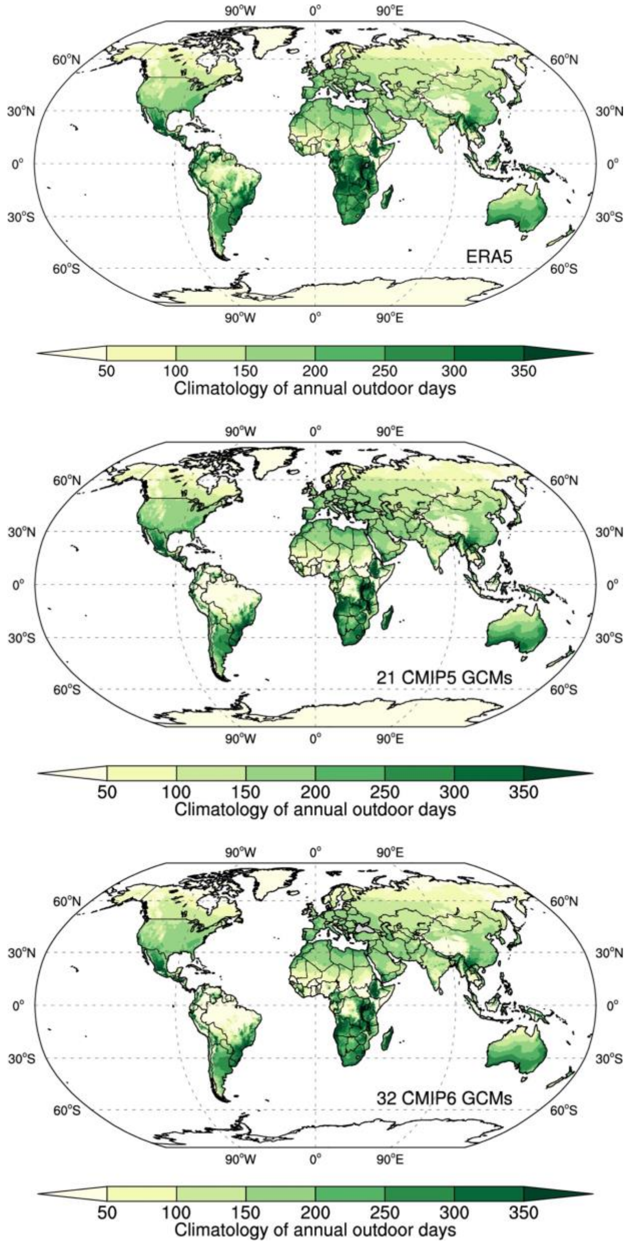

Fig. S2. Observed and simulated outdoor days. Spatial distributions of the number of annual outdoor days (days per year) for the period 1976-2005, derived from the ERA5 (top), ensemble mean of 21 NEX-GDDP-CMIP5 GCMs (middle), and ensemble mean of 32 NEX-GDDP-CMIP6 GCMs (bottom).

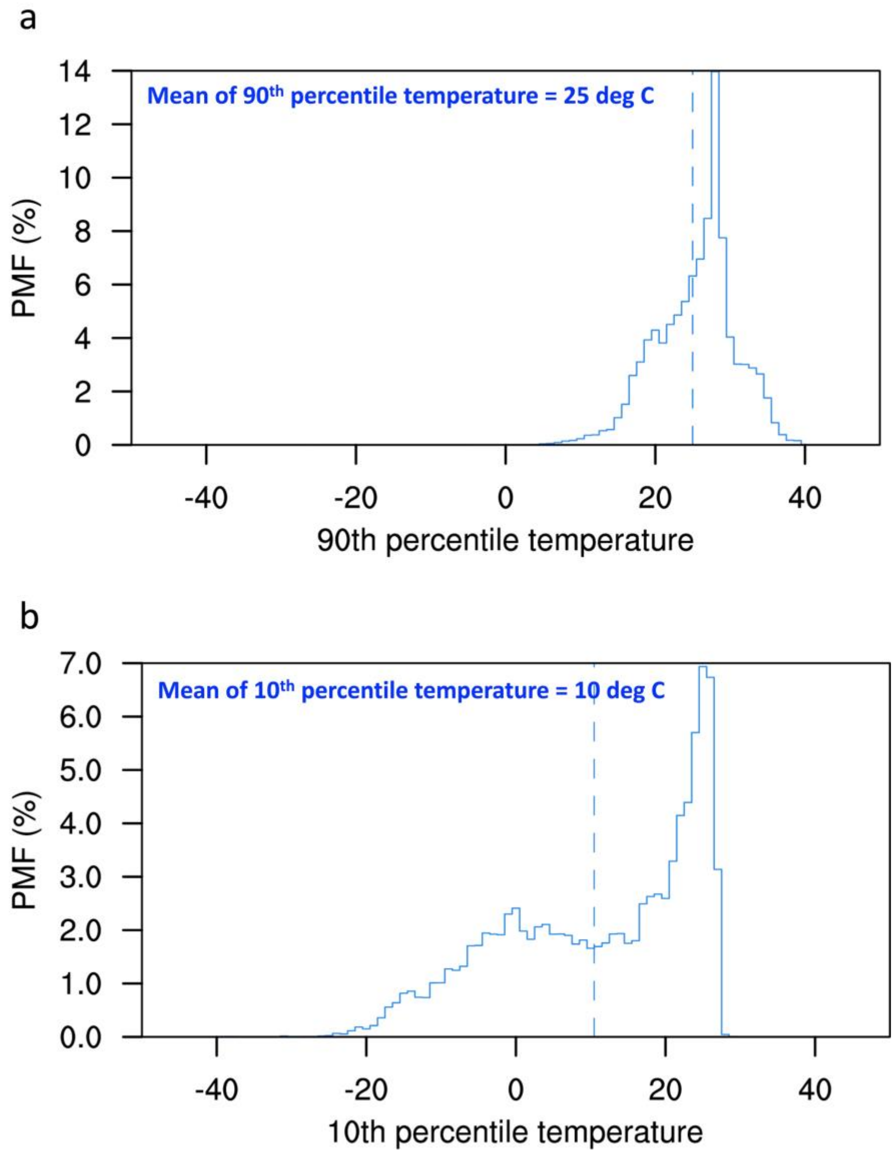

Fig. S3. Probability Mass Functions (PMF) of (a) 90th and (b) 10th percentiles of daily dry-bulb temperature in densely populated areas across the world (areas with a population density above 10 persons per square kilometer) over the period 1976–2005. The results are derived from ERA5.

Dry-bulb temperature (°C)

Relative humidity (%)

	10.0	11.0	12.0	13.0	14.0	15.0	16.0	17.0	18.0	19.0	20.0	21.0	22.0	23.0	24.0	25.0	26.0	27.0	28.0	29.0	30.0	31.0	32.0	33.0	34.0	35.0
20	2.0	2.7	3.3	4.0	4.7	5.3	6.0	6.6	7.3	7.9	8.6	9.2	9.9	10.5	11.1	11.8	12.4	13.0	13.7	14.3	14.9	15.6	16.2	16.8	17.5	18.1
25	2.6	3.3	4.0	4.6	5.3	6.0	6.7	7.4	8.1	8.8	9.4	10.1	10.8	11.5	12.1	12.8	13.5	14.2	14.8	15.5	16.2	16.8	17.5	18.2	18.9	19.5
30	3.1	3.8	4.5	5.3	6.0	6.7	7.4	8.1	8.8	9.6	10.3	11.0	11.7	12.4	13.1	13.8	14.5	15.2	15.9	16.6	17.4	18.1	18.8	19.5	20.2	20.9
35	3.6	4.4	5.1	5.9	6.6	7.4	8.1	8.8	9.6	10.3	11.1	11.8	12.5	13.3	14.0	14.8	15.5	16.2	17.0	17.7	18.5	19.2	19.9	20.7	21.4	22.1
40	4.1	4.9	5.7	6.5	7.2	8.0	8.8	9.5	10.3	11.1	11.8	12.6	13.4	14.1	14.9	15.7	16.5	17.2	18.0	18.8	19.5	20.3	21.1	21.8	22.6	23.3
45	4.6	5.4	6.2	7.0	7.8	8.6	9.4	10.2	11.0	11.8	12.6	13.4	14.2	15.0	15.8	16.6	17.4	18.2	19.0	19.8	20.6	21.3	22.1	22.9	23.7	24.5
50	5.1	5.9	6.8	7.6	8.4	9.2	10.0	10.9	11.7	12.5	13.3	14.1	15.0	15.8	16.6	17.4	18.2	19.1	19.9	20.7	21.5	22.3	23.1	24.0	24.8	25.7
55	5.6	6.5	7.3	8.1	9.0	9.8	10.7	11.5	12.3	13.2	14.0	14.9	15.7	16.6	17.4	18.3	19.1	19.9	20.8	21.6	22.5	23.3	24.1	25.0	25.9	26.8
60	6.1	7.0	7.8	8.7	9.5	10.4	11.3	12.1	13.0	13.9	14.7	15.6	16.5	17.3	18.2	19.0	19.9	20.8	21.6	22.5	23.3	24.2	25.1	26.0	26.9	27.8
65	6.6	7.4	8.3	9.2	10.1	11.0	11.8	12.7	13.6	14.5	15.4	16.3	17.2	18.1	18.9	19.8	20.7	21.6	22.5	23.3	24.2	25.1	26.0	27.0	27.9	28.8
70	7.0	7.9	8.8	9.7	10.6	11.5	12.4	13.3	14.2	15.1	16.0	17.0	17.9	18.8	19.7	20.6	21.5	22.4	23.2	24.1	25.1	26.0	27.0	27.9	28.8	29.8
75	7.5	8.4	9.3	10.2	11.1	12.1	13.0	13.9	14.8	15.8	16.7	17.6	18.5	19.4	20.4	21.3	22.2	23.1	24.0	25.0	25.9	26.9	27.8	28.8	29.7	30.7
80	7.9	8.8	9.8	10.7	11.7	12.6	13.5	14.5	15.4	16.4	17.3	18.2	19.2	20.1	21.1	22.0	22.9	23.8	24.8	25.8	26.7	27.7	28.7	29.6	30.6	31.6
85	8.4	9.3	10.3	11.2	12.2	13.1	14.1	15.0	16.0	16.9	17.9	18.9	19.8	20.8	21.7	22.7	23.6	24.5	25.5	26.5	27.5	28.5	29.5	30.5	31.4	32.4
90	8.8	9.7	10.7	11.7	12.7	13.6	14.6	15.6	16.6	17.5	18.5	19.5	20.4	21.4	22.4	23.3	24.3	25.3	26.3	27.3	28.3	29.3	30.3	31.3	32.3	33.2
95	9.2	10.2	11.2	12.2	13.1	14.1	15.1	16.1	17.1	18.1	19.1	20.1	21.0	22.0	23.0	23.9	25.0	26.0	27.0	28.0	29.0	30.0	31.0	32.0	33.0	34.0
100	9.6	10.6	11.6	12.6	13.6	14.6	15.6	16.6	17.6	18.6	19.6	20.6	21.6	22.6	23.6	24.6	25.6	26.7	27.7	28.7	29.7	30.8	31.8	32.8	33.8	34.8

Caution | Extreme Caution | Danger | Extreme Danger

Fig. S4. Four different heat-stress categories provided by the US National Weather Service. Wet-bulb temperature as a function of dry-bulb temperature and relative humidity is indicated.

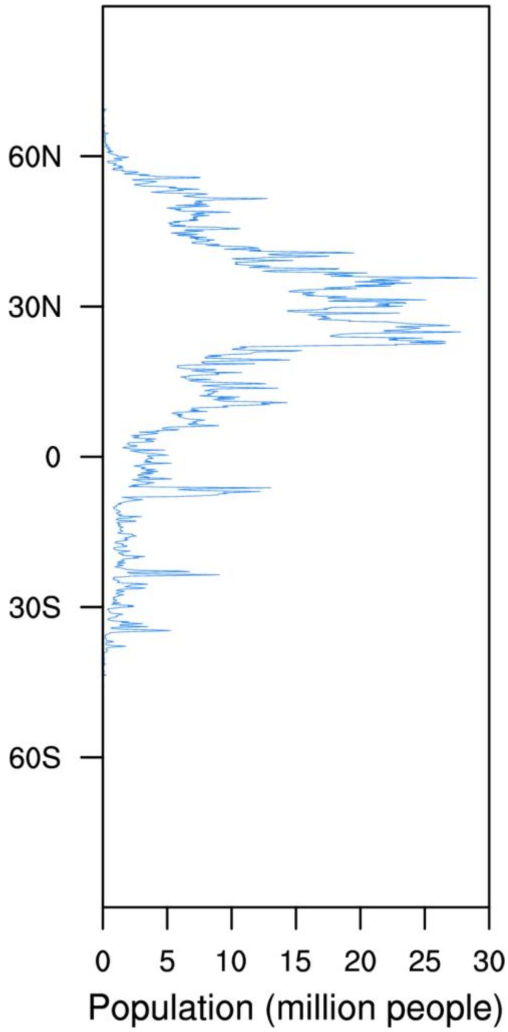

Fig. S5. The latitudinal population distribution (unit: million people) in 2000.

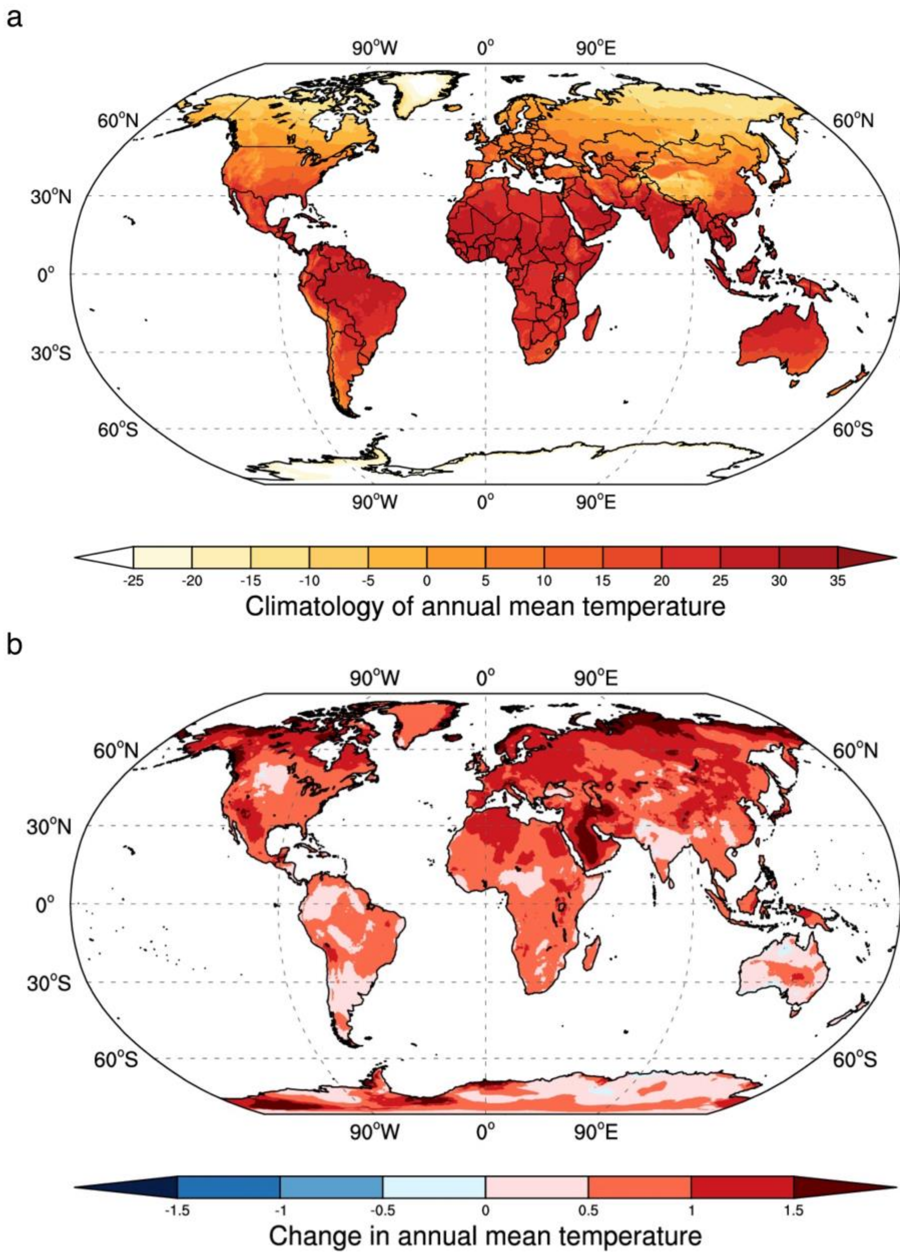

Fig. S6. Global distribution of temperature. a) Climatology of annual mean temperature for the period 1959-2021. b) Change in annual mean temperature in 1991–2020 with respect to 1961-1990. These global maps are derived from ERA5.

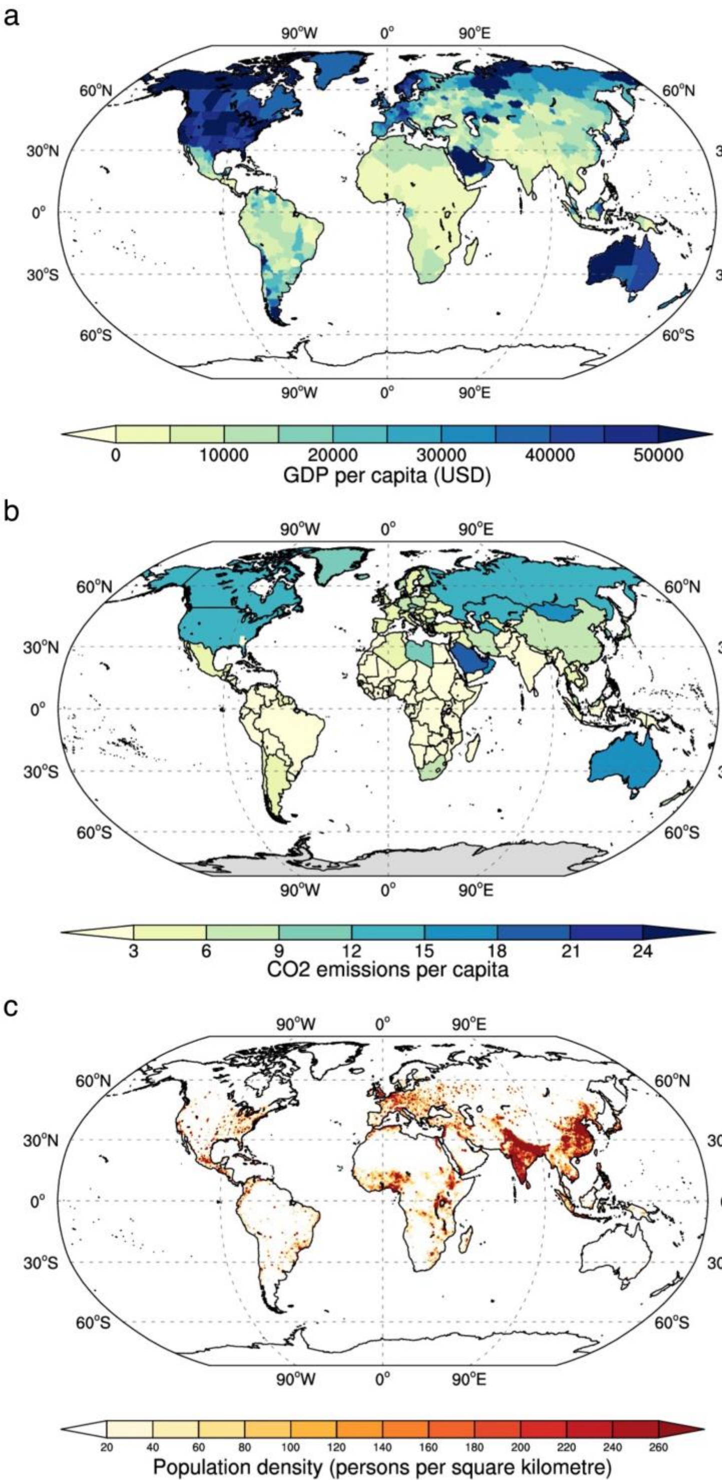

Fig. S7. Global maps of GDP, CO_2 emission, and population density. Spatial distributions of a) GDP per capita (USD), b) CO_2 emissions per capita, and c) population density (persons per square kilometer).

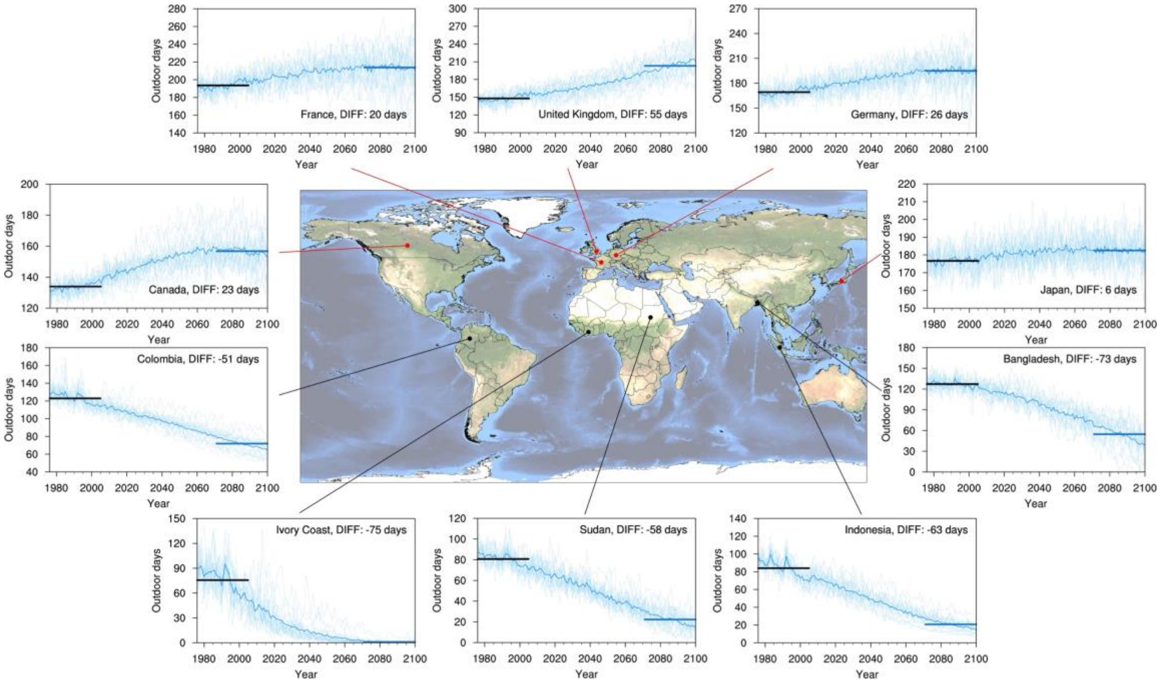

Fig. S8. Temporal evolution of outdoor days derived from NEX-GDDP-CMIP5 models. Time series of the number of annual outdoor days (days per year) over residential areas (assumed, areas with a population density above 1 person per square kilometer) derived from 21 NEX-GDDP-CMIP5 GCMs under the historical and RCP8.5 scenarios. Thick solid blue line indicates an ensemble mean of models. Horizontal black and blue lines denote the 1976-2005 mean and the 2071-2100 mean, respectively. Difference (2071–2100 minus 1976–2005) in the number of outdoor days is represented in each plot. The background image was obtained from NASA Visible Earth.

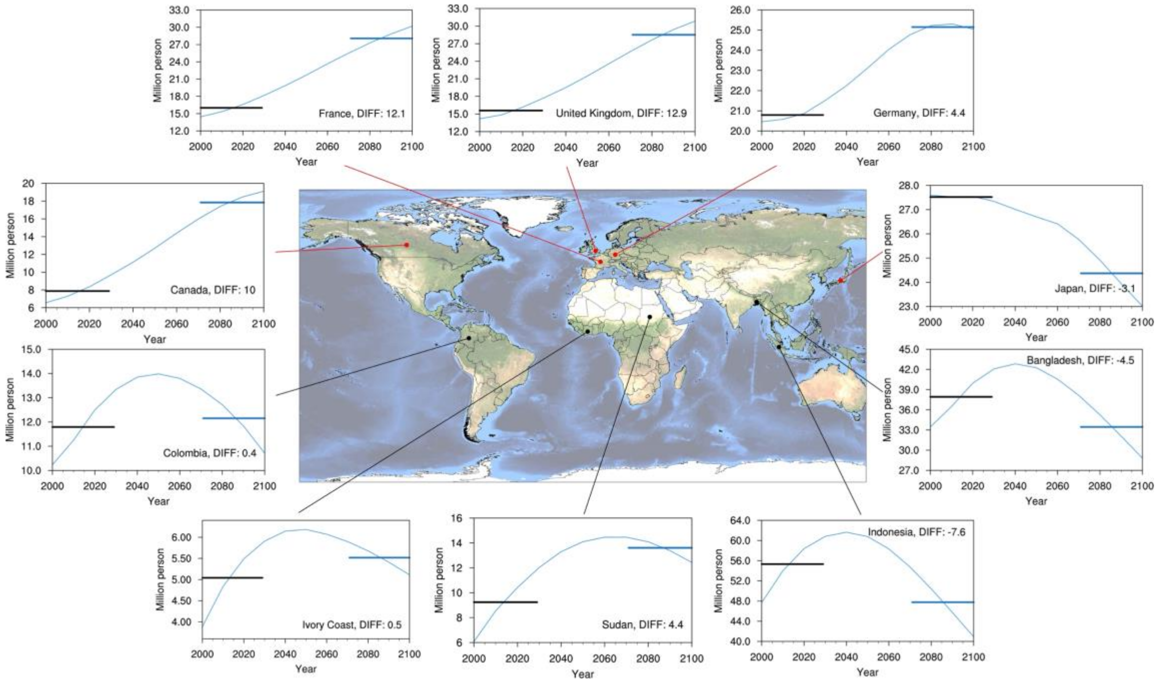

Fig. S9. Temporal evolution of population. Time series of population (million persons) over residential areas (assumed, areas with a population density above 1 person per square kilometer) derived from the SSP5 scenario. Horizontal black and blue lines denote the 2000-2029 mean and the 2071-2100 mean, respectively. Difference (2071–2100 minus 2000–2029) in population is represented in each plot. The background image was obtained from NASA Visible Earth.

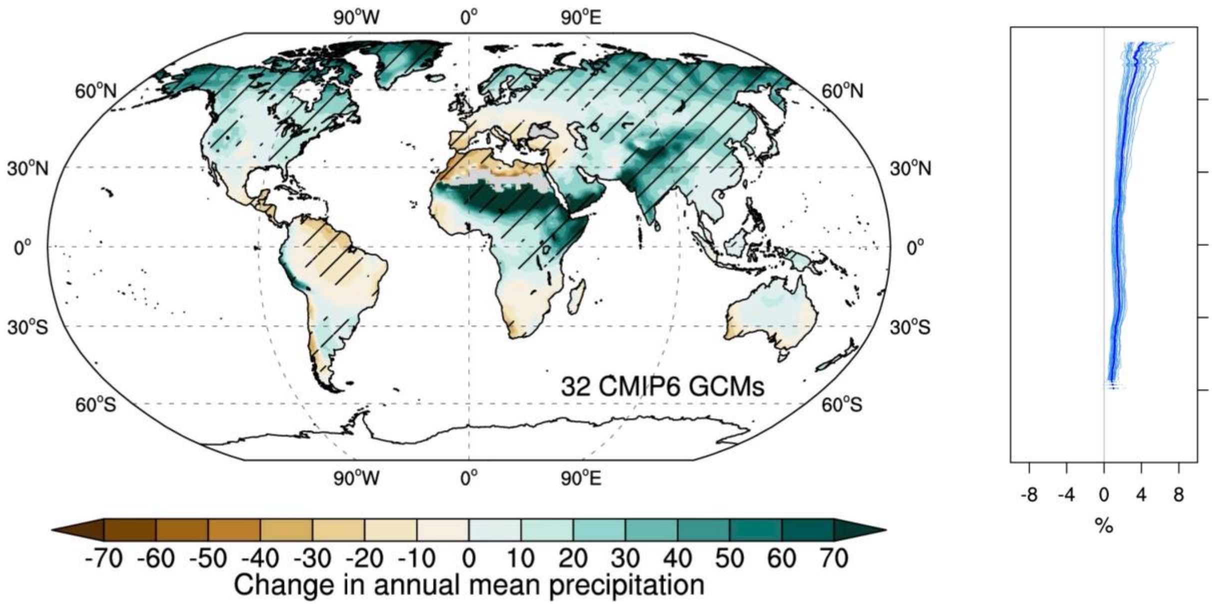

Fig. S10. Projected change in precipitation. Spatial distribution of change in annual mean precipitation (%) in 2071-2100 with respect to 1976-2005, derived from 32 NEX-GDDP-CMIP6 GCMs. Superimposed hatching indicates that more than 80% of models agree on the sign of the change. Zonal-mean change is indicated in the right panel. Thick solid blue line in the right panel indicates an ensemble mean of models.

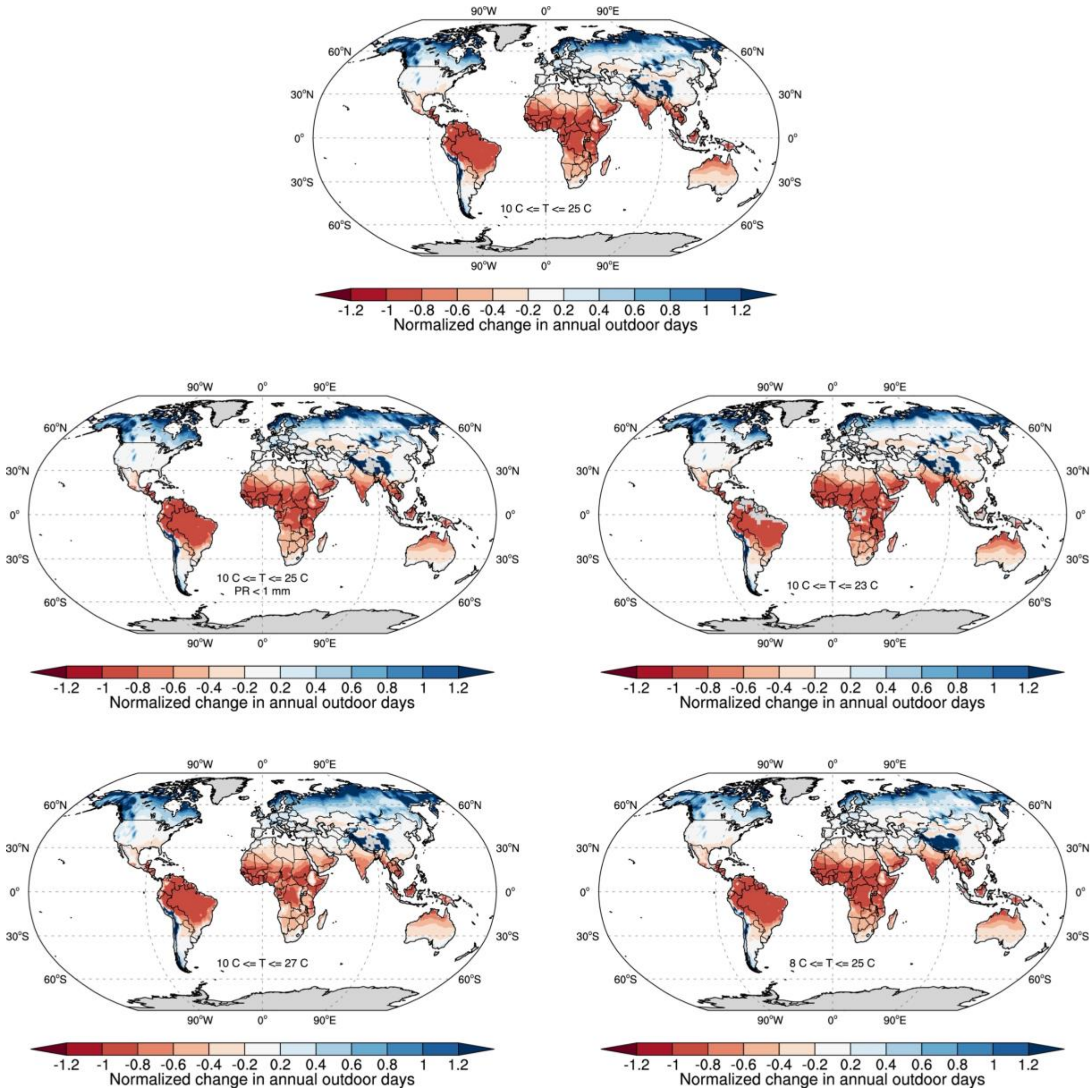

Fig. S11. Normalized change in the number of annual outdoor days with different definitions. Normalized change in the number of annual outdoor days in 2071–2100 with respect to 1976-2005. The changes are normalized by the 1976-2005 mean. Various definitions considered are indicated in each plot. Dry-bulb temperature and precipitation are indicated by T and PR, respectively. These global maps are derived from EC-Earth3-Veg-LR.

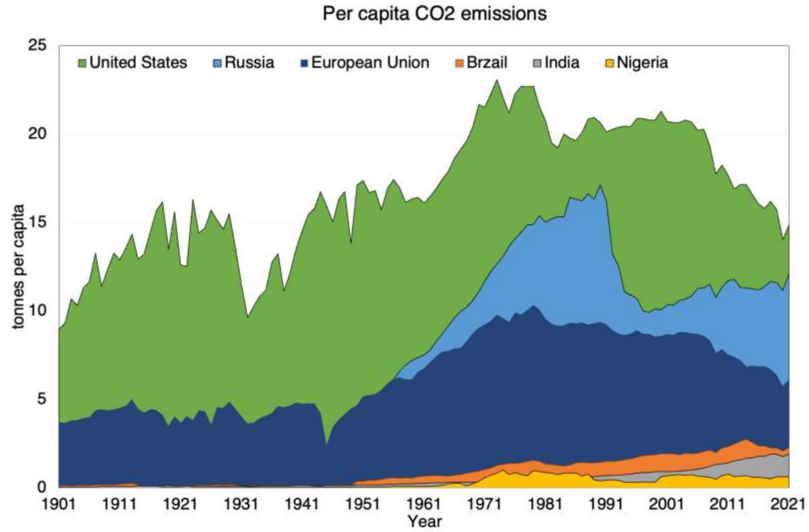

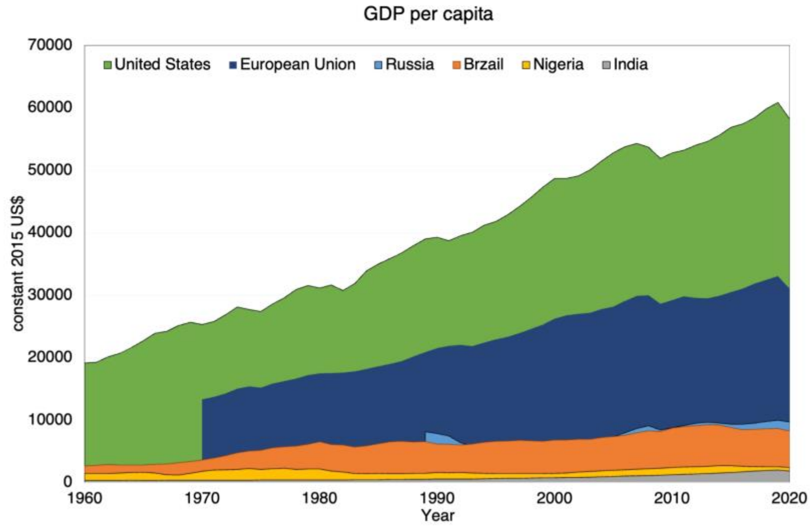

Fig. S12. Temporal evolution of CO_2 emission and GDP. Time series of (top) CO_2 emissions per capita and (bottom) GDP per capita (USD) for the United States, the European Union, Russia, Brazil, Nigeria, and India. The GDP data for European Union (Russia) is only available since 1970 (1989).

References

Boyd, E., and Coauthors, 2021: Loss and damage from climate change: A new climate justice agenda. *One Earth*, **4**, 1365–1370, https://doi.org/10.1016/j.oneear.2021.09.015.

Day, J., N. Chin, S. Sydnor, M. Widhalm, K. U. Shah, and L. Dorworth, 2021: Implications of climate change for tourism and outdoor recreation: an Indiana, USA, case study. *Climatic Change*, **169**, 29, https://doi.org/10.1007/s10584-021-03284-w.

Doelle, M., and S. Seck, 2020: Loss & damage from climate change: from concept to remedy? *Climate Policy*, **20**, 669–680, https://doi.org/10.1080/14693062.2019.1630353.

Gao, X.-J., and Coauthors, 2018: Future changes in thermal comfort conditions over China based on multi-RegCM4 simulations. *Atmospheric and Oceanic Science Letters*, **11**, 291–299, https://doi.org/10.1080/16742834.2018.1471578.

van der Geest, K., and K. Warner, 2020: Loss and damage in the IPCC Fifth Assessment Report (Working Group II): a text-mining analysis. *Climate Policy*, **20**, 729–742, https://doi.org/10.1080/14693062.2019.1704678.

Hanlon, H. M., D. Bernie, G. Carigi, and J. A. Lowe, 2021: Future changes to high impact weather in the UK. *Climatic Change*, **166**, 50, https://doi.org/10.1007/s10584-021-03100-5.

Heng, S. L., and W. T. L. Chow, 2019: How 'hot' is too hot? Evaluating acceptable outdoor thermal comfort ranges in an equatorial urban park. *Int J Biometeorol*, **63**, 801–816, https://doi.org/10.1007/s00484-019-01694-1.

IPCC, 2022: *Climate Change 2022: Impacts, Adaptation and Vulnerability. Contribution of Working Group II to the Sixth Assessment Report of the Intergovernmental Panel on Climate Change*. doi:10.1017/9781009325844.

Lin, L., E. Ge, C. Chen, and M. Luo, 2019: Mild weather changes over China during 1971–2014: Climatology, trends, and interannual variability. *Sci Rep*, **9**, 2419, https://doi.org/10.1038/s41598-019-38845-8.

Pflieger, G., 2023: COP27: One step on loss and damage for the most vulnerable countries, no step for the fight against climate change. *PLOS Clim*, **2**, e0000136, https://doi.org/10.1371/journal.pclm.0000136.

Spagnolo, J., and R. de Dear, 2003: A field study of thermal comfort in outdoor and semi-outdoor environments in subtropical Sydney Australia. *Building and Environment*, **38**, 721–738, https://doi.org/10.1016/S0360-1323(02)00209-3.

Warner, K., and M. Weisberg, 2023: A funding mosaic for loss and damage. *Science*, **379**, 219–219, https://doi.org/10.1126/science.adg5740.

van der Wiel, K., S. B. Kapnick, and G. A. Vecchi, 2017: Shifting patterns of mild weather in response to projected radiative forcing. *Climatic Change*, **140**, 649–658, https://doi.org/10.1007/s10584-016-1885-9.

Wu, J., X. Gao, F. Giorgi, and D. Chen, 2017: Changes of effective temperature and cold/hot days in late decades over China based on a high resolution gridded observation dataset. *International Journal of Climatology*, **37**, 788–800, https://doi.org/10.1002/joc.5038.

Zhang, J., Q. You, G. Ren, and S. Ullah, 2022: Projected changes in mild weather frequency over China under a warmer climate. *Environ. Res. Lett.*, **17**, 114042, https://doi.org/10.1088/1748-9326/ac9c70.